International Journal of Heat and Mass Transfer 52 (2009) 1965–1970

Contents lists available at ScienceDirect

International Journal of Heat and Mass Transfer

journal homepage: www.elsevier.com/locate/ijhmt

Unsteady thin-film flow over a heated stretching sheet

Bidyut Santra [a], Bhabani S. Dandapat [b,*]

[a] Department of Mathematics, Jangipur College, Murshidabad 742 213, India
[b] Department of Mathematics, Sikkim Manipal Institute of Technology, Majitar, Rangpo, East Sikkim 737 132, India

ARTICLE INFO

Article history:
Received 17 April 2008
Received in revised form 5 September 2008
Available online 29 December 2008

Keywords:
Thin liquid film
Stretching sheet
Free surface flow
Thermocapillary flow
Heat transfer

ABSTRACT

The unsteady flow in a thin viscous liquid film over a heated horizontal stretching surface are analyzed considering the stretching velocity and the temperature distribution in their general forms. An evolution equation for the film thickness, that retains the convective heat transport effects, is derived using long-wave theory of thin liquid film and is solved numerically for some representative values of non-dimensional parameters. It is observed that the thermocapillary effects are responsible in shaping the film thickness. Further the thermocapillary effects are more pronounced for lower values of Prandtl number and Biot number.

1. Introduction

The flow and heat transfer phenomena of a viscous liquid over a stretching surface has promising applications in a number of technological processes such as metal and polymer extrusion, continuous casting, drawing of plastic sheets, etc. In these processes, quality of the final product greatly depends on the rate of cooling. Crane [1] first studied the steady two-dimensional boundary layer flow due to the stretching of a flat elastic sheet. Later on several researchers, see e.g. the references cited in [2], have explored various aspects of the accompanying heat transfer occurring in the infinite fluid medium surrounding the stretching sheet. Wang [3] first studied the hydrodynamics of a finite fluid medium on a stretching sheet, in which he restricted the motion to a specified family of time dependence and reduced the boundary layer equations to a nonlinear ordinary differential equation by means of a similarity transformation. Andersson et al. [2] analyzed the heat transfer of a Newtonian liquid film on an unsteady stretching surface. Dandapat et al. [4] later studied the influence of thermocapillarity on the flow and heat transfer of the same problem. Chen [5] also studied it in case of power-law fluid. Recently, Dandapat et al. [6] have studied the effects of the variation of fluid properties with temperature on the same flow that studied earlier by Dandapat et al. [4]. The tacit planarity assumption of film thickness made in the above studies may not be valid while the influence of the thermocapillarity is considered. This is due to the fact that thermocapillary flow itself deforms the free surface.

Dandapat et al. [7] and Dandapat and Maity [8] have studied the development of thin film over a stretching sheet with non-planar film thickness at the onset of stretching. In these studies the Navier–Stokes equations are solved analytically using a combination of the matched asymptotic method and the method of characteristics to predict the variation of film thickness with space and time. In these studies linear variation of the stretching sheet were considered. Recently, Santra and Dandapat [9] have studied the development of thin liquid film flow over a sheet that may be stretched under different nonlinear stretching assuming non-planar film thickness.

In the present investigation we have removed the restriction of planarity as well as the linear stretching to study the effects of heat-transfer and thermocapillarity. The rest of the paper is organized as follows. In the next section, we formulate the governing equations and after non-dimensionalization, the evolution equation for the film thickness is obtained using long wave theory of thin liquid films. The numerical technique to solve the evolution equation is described in Section 3. The results and discussions of numerical computations are reported in Section 4. Finally, conclusions are drawn in Section 5.

2. Mathematical formulation

2.1. Basic governing equations

We consider a non-planar, Newtonian, incompressible liquid film on a heated flat elastic sheet as shown schematically in Fig. 1. The x-axis is chosen along the plane of the sheet and the z-axis is taken normal to the plane. We assume that the surface

* Corresponding author. Tel.: +91 9433391227; fax: +91 3592 246 112.
E-mail address: bsdandapat@rediffmail.com (B.S. Dandapat).

0017-9310/$ - see front matter © 2008 Elsevier Ltd. All rights reserved.
doi:10.1016/j.ijheatmasstransfer.2008.09.036

Nomenclature

B	Biot number, $\alpha h_0/k$
Ca	Capillary number, ε^2/S
c_p	specific heat at constant pressure (J kg^{-1} K^{-1})
Fr	modified Froude number, gh_0^3/ν^2
$\mathbf{g}$	gravitational acceleration (m s^{-2})
g	vertical component of gravitational acceleration (m s^{-2})
h	film thickness (m)
h_0	characteristic length scale in the vertical direction (m)
k	thermal conductivity (W m^{-1} K^{-1})
L	characteristic length scale in the horizontal direction (m)
M_w	effective Marangoni number, $h_0\gamma(T_{s_0}-T_a)/\rho\nu^2$
$\mathbf{n}$	unit normal vector on the interface
Pr	Prandtl number, $\rho c_p\nu/k$
p	pressure (kg m^{-1} s^{-2})
S	surface tension parameter, $\varepsilon^2\sigma_a h_0/\rho\nu^2$
$\mathbf{t}$	tangential vector on the interface
t	time (s)
T	temperature (K)
U	sheet velocity (m s^{-1})
$\mathbf{V}$	velocity of the fluid (m s^{-1})
u	horizontal velocity component (m s^{-1})
w	vertical velocity component (m s^{-1})
x	horizontal coordinate (m)
z	vertical coordinate (m)

Greek symbols

α	rate of heat transport (W m^{-2} K^{-1})
ε	aspect ratio, h_0/L
γ	constant (K^{-1})
Θ	dimensionless temperature of the stretching sheet
ν	kinametic viscosity (m^2 s^{-1})
ρ	density (kg m^{-3})
σ	surface tension (kg s^{-2})
τ	stress tensor
ψ	stream function

Subscripts

i	interface
a	ambient
s	sheet

Superscript

*	nondimensional variable (from Eq. (10) and onwards all the variables are in their nondimensional form)

at $z=0$ starts stretching from rest and within a very short time ($t=0^+$) it attains the stretching velocity $u=U(x)$. The liquid is assumed to be non-volatile and thin so that evaporation and buoyancy effect can be neglected. Further we assume that the liquid properties are constant, except the surface tension that varies linearly with temperature $\sigma=\sigma_a-\gamma(T_i-T_a)$, where T_i is the interfacial temperature and T_a is the ambient gas temperature far from liquid–gas interface. The motion of the fluid is governed by

$$\nabla\cdot\mathbf{V}=0, \tag{1}$$

$$\mathbf{V}_t+(\mathbf{V}\cdot\nabla)\mathbf{V}=-\nabla p/\rho+\nu\nabla^2\mathbf{V}+\mathbf{g} \tag{2}$$

$$\rho c_p[T_t+(\mathbf{V}\cdot\nabla)T]=k\nabla^2T, \tag{3}$$

where $\mathbf{V}$ and $\mathbf{g}$ denote the fluid velocity and acceleration due to gravity having (u,w) and $(0,-g)$ as the respective components along x- and z-directions and p, ρ, ν, c_p and k represent the pressure, density, kinematic viscosity, heat capacity at constant pressure and thermal conductivity of the fluid, respectively.

The boundary conditions on the stretching sheet $z=0$, are no-slip, no penetration and the imposed sheet temperature distribution, respectively,

$$u(t,x,0)=U(x),\quad w(t,x,0)=0,\quad T=T_s(x), \tag{4}$$

where $T_s(x)$ is the imposed sheet temperature. On the interface, $z=h(x,t)$, the boundary conditions constitute the balance of normal stress with the surface tension times of curvature, balance of tangential stress with the thermal stress, along with the Newton's law of cooling and the kinematic condition given by:

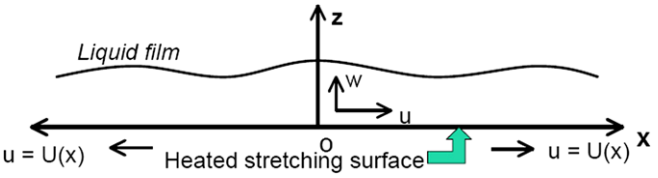

Fig. 1. Schematic diagram of the flow problem.

$$p_a+\mathbf{n}\cdot\tau\cdot\mathbf{n}=-\nabla\cdot\mathbf{n}\sigma, \tag{5}$$

$$\mathbf{t}\cdot\tau\cdot\mathbf{t}=\mathbf{t}\cdot\nabla\sigma, \tag{6}$$

$$-k\nabla T\cdot\mathbf{n}=\alpha(T-T_a), \tag{7}$$

$$h_t=w-uh_x, \tag{8}$$

where τ is the stress tensor for the liquid, $\mathbf{n}$ and $\mathbf{t}$ are unit normal and tangential vectors on the interface, p_a is the pressure of the ambient gas phase and α is the rate of heat transport from the liquid to the ambient gas phase.

The initial conditions are:

$$u(0,x,z)=0,\quad w(0,x,z)=0,\quad h(x,0)=\delta(x),\quad T=T_a.$$

2.2. Scaling

Eqs. (1)–(8) can be expressed in terms of their dimensionless form by using the following variables:

$$\begin{aligned}&x=Lx^*,\quad (z,h)=h_0(z^*,h^*),\quad (u,U)=(\nu/h_0)(u^*,U^*),\\ &w=(\varepsilon\nu/h_0)w^*,\quad t=\left(h_0^2/\varepsilon\nu\right)t^*,\quad p=\left(\rho\nu^2/\varepsilon h_0^2\right)p^*+p_a,\\ &T=T_a+(T_{s_0}-T_a)T^*\end{aligned} \tag{9}$$

where L and h_0 are the characteristic length scale in the horizontal and vertical direction, respectively, $\varepsilon=h_0/L\ll 1$ is the aspect ratio and T_{s_0} is the sheet temperature at the origin. Finally, after dropping the asterisk, we obtain

$$u_x+w_z=0, \tag{10}$$

$$\varepsilon(u_t+uu_x+wu_z)=-p_x+\varepsilon^2u_{xx}+u_{zz}, \tag{11}$$

$$\varepsilon^3(w_t+uw_x+ww_z)=-p_z+\varepsilon^4w_{xx}+\varepsilon^2w_{zz}-\varepsilon Fr, \tag{12}$$

$$\varepsilon Pr(T_t+uT_x+wT_z)=\varepsilon^2T_{xx}+T_{zz}. \tag{13}$$

The boundary conditions, at $z=0$ becomes

$$u(t,x,0)=U(x),\quad w(t,x,0)=0,\quad T=\Theta(x), \tag{14}$$

where $\Theta(x)=(T_s-T_a)/(T_{s_0}-T_a)$.

On the interface $z=h(x,t)$:

$$-p+2\frac{\varepsilon^2}{\left(1+\varepsilon^2h_x^2\right)}\left[\varepsilon^2u_xh_x^2+w_z-u_zh_x-\varepsilon^2w_xh_x\right]$$
$$=\varepsilon S(1-M_wCaT)\left(1+\varepsilon^2h_x^2\right)^{-3/2}h_{xx}, \tag{15}$$

$$\left[2\varepsilon^2h_x(w_z-u_x)+\left(u_z+\varepsilon^2w_x\right)\right]\left(1-\varepsilon^2h_x^2\right)$$
$$=-\varepsilon M_w(T_x+h_xT_z)\left(1+\varepsilon^2h_x^2\right)^{1/2}, \tag{16}$$

$$T_z-\varepsilon^2h_xT_x=-B\left(1+\varepsilon^2h_x^2\right)^{1/2}T, \tag{17}$$

$$h_t=w-uh_x. \tag{18}$$

The initial conditions at $t=0$

$$u(0,x,z)=0,\quad w(0,x,z)=0,\quad h(x,0)=\delta(x),\quad T=0.$$

Here $Fr=gh_0^3/v^2$, $Pr=\rho c_pv/k$, $S=\varepsilon^2\sigma_ah_0/\rho v^2$, $M_w=h_0\gamma(T_{S_0}-T_a)/\rho v^2$, $Ca=\varepsilon^2/S$ and $B=\alpha h_0/k$ are the modified Froude number, Prandtl number, surface tension parameter, effective Marangoni number, Capillary number and Biot number, respectively.

2.3. Derivation of the evolution equation

To obtain the evolution equation for film thickness, we expand the dependent variables as follows:

$$(u,w,p)=(u_0,w_0,p_0)+\varepsilon(u_1,w_1,p_1)+\varepsilon^{2-n}(u_2,w_2,p_2)+\cdots, \tag{19}$$

$$T=T_0+\varepsilon^{1-n}T_1+\cdots, \tag{20}$$

where $0<n<1$.

In our analysis we retain terms up to $O(\varepsilon^{2-n})$ and neglect terms of $O(\varepsilon^2)$ and higher to capture the effects of Large Prandtl number on film thinning, in a similar way as done by Trevelyan and Kalliadasis [10] and Trevelyan et al. [11] in a different context of falling liquid films. In the present analysis Prandtl number is assumed to be $Pr=O(\varepsilon^{-n})$. We also assume M_w, Fr and Bi to be of $O(1)$. The asymptotic analysis is carried out by substituting (19) and (20) into the system of Eqs. (10)–(18) and collecting different orders of ε. Finally, solving these set of equations simultaneously we obtain the velocity components u and w up to $O(\varepsilon^{2-n})$ and the temperature T up to $O(\varepsilon^{1-n})$. The final solutions read as:

$$T=\left(\frac{1+B(h-z)}{1+Bh}\right)\Theta(x)+\varepsilon Pr\left[\frac{U\Theta_x}{2}\left\{z^2-\left(\frac{2+Bh}{1+Bh}\right)hz\right\}-\left\{\frac{B^2\Theta U_xh}{6(1+Bh)^2}+\frac{B(U\Theta_x-U_x\Theta)}{6(1+Bh)}\right\}\left\{z^3-\left(\frac{3+Bh}{1+Bh}\right)h^2z\right\}\right] \tag{21}$$

and

$$\Psi=Uz+\varepsilon\left[(UU_x+Frh_x-Sh_{xxx})\left(\frac{z^3}{6}-\frac{hz^2}{2}\right)-M_w\left(\frac{\Theta(x)}{1+Bh}\right)_x\frac{z^2}{2}\right]+\varepsilon^2PrM_w\left[-\frac{B^2}{3}\left(\frac{\Theta U_xh^4}{(1+Bh)^3}\right)_x+\frac{B}{3}\left(\frac{(U_x\Theta-U\Theta_x)h^3}{(1+Bh)^2}\right)_x+\frac{1}{2}\left(\frac{U\Theta_xh^2}{1+Bh}\right)_x\right]\frac{z^2}{2}. \tag{22}$$

In deriving Eq. (22) we have used the relations $u=\Psi_z$ and $w=-\Psi_x$. Here Ψ is the stream function. It is to be noted here that the above solution does not satisfy the initial conditions due to large characteristics time scale considered in the analysis. Using (22) in the kinematic boundary condition (18), the free surface evolution equation is obtained as follows:

$$h_t+F(h)=0, \tag{23}$$

where

$$F(h)=\frac{\partial}{\partial x}\left[(Uh)+\varepsilon\left\{-\frac{1}{3}(UU_xh^3)-\frac{Fr}{3}(h^3h_x)+\frac{S}{3}(h^3h_{xxx})-\frac{M_w}{2}\left(h^2\left(\frac{\Theta}{1+Bh}\right)_x\right)\right\}+\varepsilon^2PrM_w\left\{\frac{B}{6}\left(\frac{U_x\Theta h^3}{(1+Bh)^3}\right)_xh^2+\frac{1}{12}\left(\frac{U\Theta_x(3+Bh)h^2}{(1+Bh)^2}\right)_xh^2\right\}\right]$$

3. Numerical solution

The evolution equation for film thickness is solved numerically by using a combination of modified Euler method, the Newton–Kantorovich method, and the finite difference method as described by Oron and Bankoff [12]. The evolution equation (23) is discretized in time using modified Euler method in the form

$$h^{n+1}-h^n=(\Delta t/2)\cdot[-F(h^n)-F(h^{n+1})], \tag{24}$$

where Δt is the time step and h^n represent the solution of the evolution equation obtained at the time $t_n=n\Delta t\cdot F(h^{n+1})$, is then linearized by

$$F(h^{n+1})=F(h^n)+F_h^{(n)}(h^{n+1}-h^n), \tag{25}$$

where $F_h^{(n)}$ is the Frechet differential operator evaluated at time t_n. Combining (24) and (25) one can get

$$\left(I+\frac{\Delta t}{2}F_h\right)u=-\Delta t\cdot F(h^n), \tag{26}$$

where $u=h^{n+1}-h^n$ is the difference between the solutions calculated for consecutive times, I is the identity operator and

$$F_hu=(Uu)_x+\varepsilon\left[-\left(UU_xh^2u\right)_x-\frac{Fr}{3}\left(h^3u_x+3h^2h_xu\right)_x+\frac{S}{3}\left(3h^2h_{xxx}u+h^3u_{xxx}\right)_x+\frac{BM_w}{2}\left\{h^2\left(\frac{uT_i}{1+Bh}\right)_x\right\}_x-M_w(huT_{ix})_x\right]+\varepsilon^2PrM_w\left[\frac{B}{3}\left\{\left(\frac{U_x\Theta h^3}{(1+Bh)^3}\right)_xhu\right\}_x+\frac{B}{2}\left\{\left(\frac{U_x\Theta h^2u}{(1+Bh)^4}\right)_xh^2\right\}_x+\frac{1}{6}\left\{\left(\frac{U\Theta_x(3+Bh)h^2}{(1+Bh)^2}\right)_xhu\right\}_x+\frac{1}{12}\left\{\left(\frac{U\Theta_x(6+3Bh+B^2h^2)hu}{(1+Bh)^3}\right)_xh^2\right\}_x\right].$$

In the above equation, $T_i=T_i(x,t)$ denotes the zeroth order contribution of liquid–gas interface temperature. The last equation which is a linear ordinary differential equation in terms of the variable $u(x,t)$, is then discretized using a central difference scheme and linear interpolation for half nodes accurate to $O(\Delta x^2)$ where Δx is the spatial step. Use of modified Euler method during time discretization, gives precision of $O(\Delta t^2)$. The conservative form is used during discretization. The sets of linear algebraic equations resulting form the discretization of Eq. (26), forms a pentadiagonal system with three corner elements and are solved directly by modified Thomas algorithm. At the origin we apply the symmetry conditions $h_x=0$ and $h_{xxx}=0$. At the end, we assume that same sheet temperature profile continues beyond the computed domain. We further assume that the film surface has the same gradient just after the end point of the computed zone, i.e., $h_x|_{j=N}=h_x|_{j=N+1}=h_x|_{j=N+2}$ where N denotes the number of spatial step. The grids of 250–500 points suffices the spatial convergence of the solutions. It is to be noted here that due to the symmetry of the problem

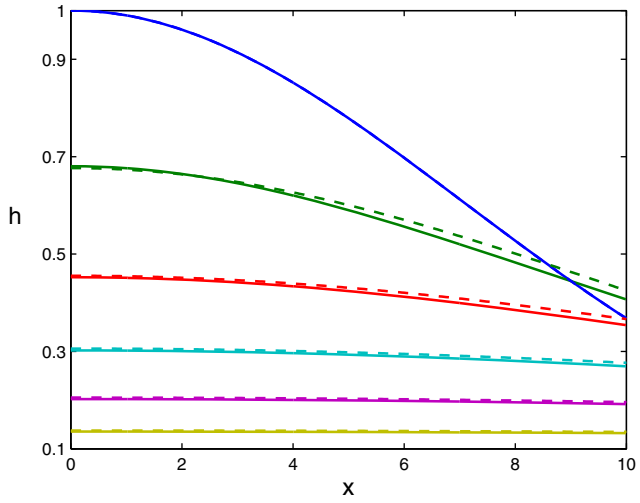

Fig. 2. Comparison of numerical solution (dash line) with analytical solution (solid line) given in Ref. [7] for non-uniform film profile $\delta(x) = \exp(-x^2/100)$ from time $t = 0.0$ to $t = 2.0$ with increments of 0.4. Numerical solution corresponds to $\varepsilon = 0.1$.

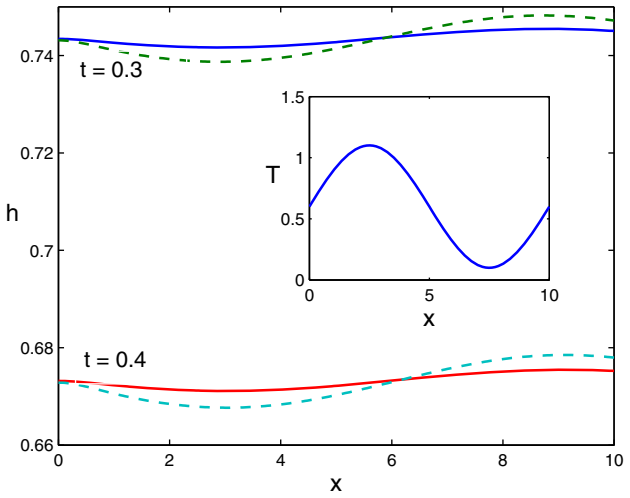

Fig. 4. Film profile h versus x at $t = 0.3$ and.4 for $M_w = 4$ (solid line) and 10 (dash line). Sheet temperature $\Theta = 0.6 + 0.5\sin(2\pi x/10)$ (shown in the inset), initial film profile $\delta(x) = 1$, sheet velocity $U = x$, $\varepsilon = 0.05$, $S = 2$, $Fr = 2$, $Bi = 1$ and $Pr = 1$.

about the y-axis, it is expected that one can obtain the solution for $x < 0$ as a mirror image of the solution for $x > 0$. Further we like to emphasize that the non-dimensional parameters that we use in the computations are not exact; rather they permit us to mark different physical effects and examine their influences.

4. Results and discussion

Fig. 2 represents the variation of film height with x at different time steps. The continuous line represents the analytic solution obtained by Dandapat et al. [7], and the dashed line represents the numerical solution obtained by the above numerical method. It is to be noted here that both the solutions represent the case of linear stretching for isothermal situation and these solutions agree well.

Fig. 3 shows the film profiles for linear and non-linear stretching velocity of the bottom sheet for two different values of the thermocapillary parameter (effective Marangoni number) M_w. From this figure it is clear that the film profile is mainly guided by the type of stretching applied to the bottom sheet. The effect of thermocapillarity are almost similar to all the three stretching cases. Thus in the subsequent analysis on the heat transfer phenomena we consider the linear stretching case only.

Figs. 4 and 5 show the thermocapillary effect for a sinusoidal temperature distribution on the film height variation along the stretching direction at different time steps. It is clear from the figures that film height decreases or increases at the higher or lower temperature zones due to thermocapillary effect. Further it is observed that the deformation is more for the case of high Marangoni number (represented by dash line for $M_w = 10$) than that for the low Marangoni number (represented by solid line for $M_w = 4$), obviously due to the higher variation of surface tension with temperature. Fig. 6 shows the variation of free surface temperature with x at different Prandtl numbers under the same sheet temperature distribution. Fig. 7 represents gradual development of film height at different time for a smoothed step function type temperature distribution. It is clear from the figure that free surface is deformed due to thermocapillarity and the deformation is advected by the flow in the stretching direction.

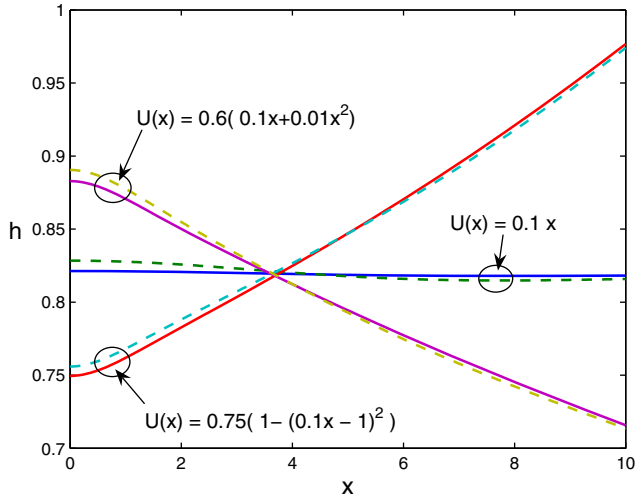

Fig. 3. Film profile h versus x at $t = 2.0$ for $M_w = 2$ (solid line) and $M_w = 8$ (dash line), under different stretching velocity. Sheet temperature $\Theta = 1 - e^{-x^2/33}$, is assumed to be fixed for all cases along with the initial film profile $\delta(x) = 1$, $\varepsilon = 0.05$, $S = 2$, $Fr = 2$ and $Pr = 1$.

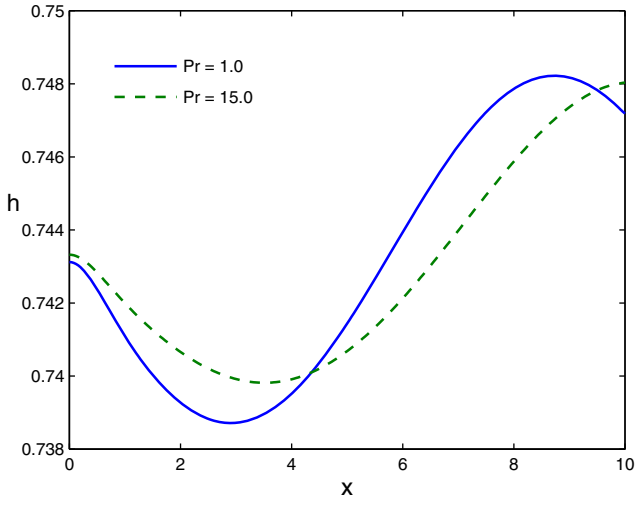

Fig. 5. Film profile h versus x at $t = 0.3$ for $Pr = 1$ and 15. Sheet temperature $\Theta = 0.6 + 0.5\sin(2\pi x/10)$, initial film profile $\delta(x) = 1$, sheet velocity $U = x$, $\varepsilon = 0.05$, $S = 2$, $Fr = 2$, $Bi = 1$ and $M_w = 10$.

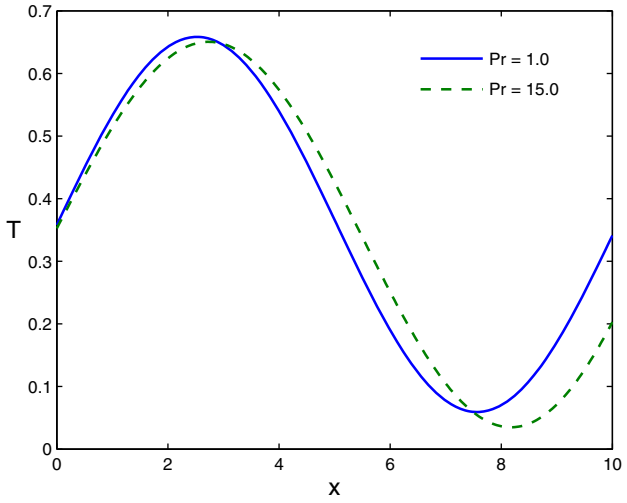

Fig. 6. Free surface temperature T versus x at $t = 0.3$ for $Pr = 1$ and 15. Sheet temperature $\Theta = 0.6 + 0.5\sin(2\pi x/10)$, initial film profile $\delta(x) = 1$, sheet velocity $U = x$, $\varepsilon = 0.05$, $S = 2$, $Fr = 2$, $Bi = 1$ and $M_w = 10$.

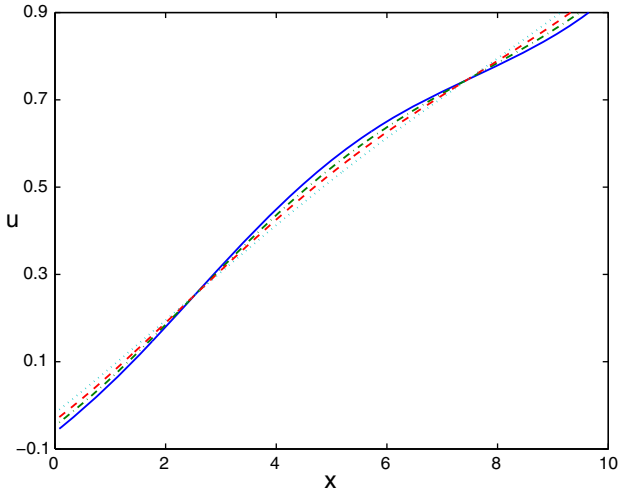

Fig. 8. Horizontal component of velocity u versus x at time $t = 2$ (solid line), 4 (dash-dot line), 6 (dash line) and 10 (dotted line) when sheet temperature $\Theta = 0.6 + 0.5\sin(2\pi x/10)$, initial film profile $\delta(x) = 1$, sheet velocity $U = 0.1x$, $\varepsilon = 0.05$, $S = 2$, $Fr = 2$, $Bi = 1$ and $M_w = 10$.

Variation of the horizontal component of velocity u at the free surface with x is presented in Fig. 8 for different time steps. It is evident from the figure that u gradually attain linear stretching speed at large time. Fig. 9 represents the streamline patterns within the fluid. Fig. 10 shows the effect of different bottom surface temperature distribution on the horizontal component of velocity (u) along the vertical direction under different Prandtl numbers. Curve B represents the case when the bottom surface temperature is uniform. In this case, no effective thermocapillary force acts on the free surface and u decreases in the upwards direction from the sheet velocity. Curve A represents the case when the bottom surface temperature is higher at the origin and it decreases in the x-direction and thus thermocapillary force acts in the direction of stretching. The fluid layer just below the free surface is dragged along by the top layer due to viscous shear and resulting a local velocity minimum inside the liquid film. The surface velocity in this case may even exceed the sheet velocity as captured in the figure. This result were also earlier found by Dandapat et al. [4]. While curve C shows the effect of increasing bottom temperature on u. In this case the thermocapillary force acts in the opposite direction of stretching and thus u decreases rather quickly from the sheet velocity as one approaches towards the free surface.

The effect of Biot number on the heat transfer and film profile are displayed in Figs. 11 and 12, respectively, for low and high Pr. The Biot number is a measure of the heat transport from the liquid to the surrounding medium in comparison to the heat transport within the liquid. As Bi increases, more heat is transferred to the surrounding environment causing decrease in the temperature difference along stretching direction. As a result the thermocapillary action decreases. So the deformation of the free surface is lesser in case of higher Bi and it is illustrated in Fig. 12. Also we notice that as Pr increases the temperature difference in the stretching direction decreases for any Bi and the deformation of the free surface due to thermocapillarity also reduces.

5. Conclusions

Flow and heat transfer phenomena over a heated stretching sheet are analyzed by considering the general functional forms

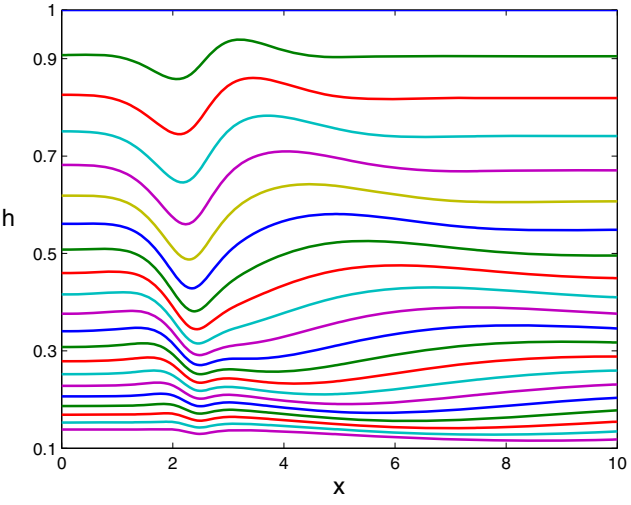

Fig. 7. Evolution of the film profile h for a smoothed step function type temperature distribution $\Theta = 0.5[1.1 + \tanh\{35(2.5 - x)/10\}]$ from $t = 1$ to $t = 20$ with increments of 1. Here initial film profile $\delta(x) = 1$, sheet velocity $U = 0.1x$, $\varepsilon = 0.05$, $S = 2$, $Fr = 2$, $Bi = 1$, $M_w = 4$.

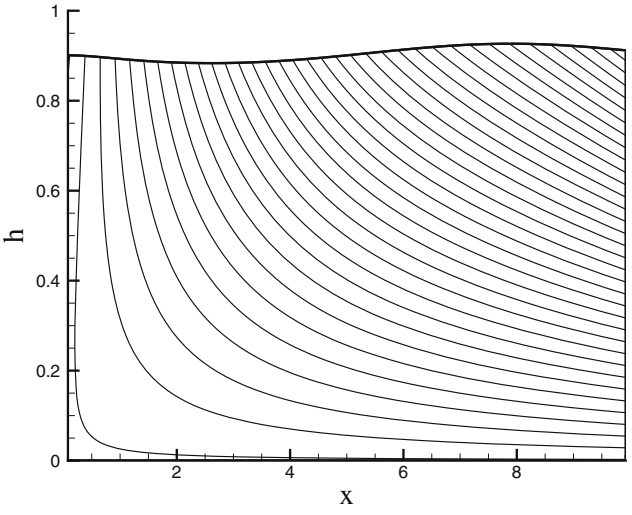

Fig. 9. Stream lines pattern at time $t = 4$. Other information are same as in Fig. 8.

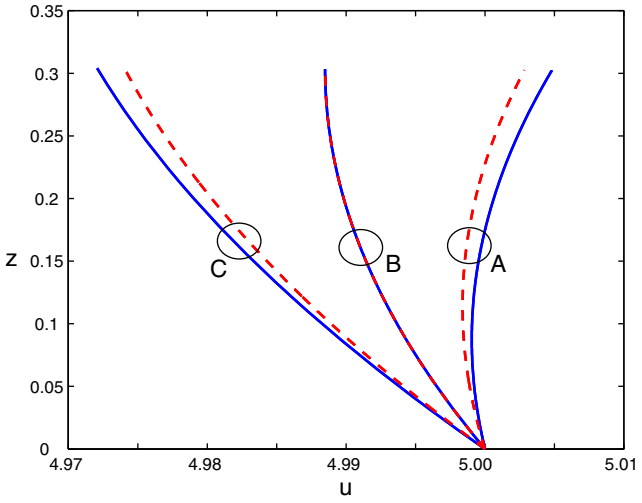

Fig. 10. Horizontal component of velocity profile at $x = 5$ across the film height for three different temperature distributions: $\Theta = e^{-x^2/33}$ (marked A), $\Theta = 0.5$ (marked B) and $\Theta = 1 - e^{-x^2/33}$ (marked C) and for $Pr = 1$ (solid line) and $Pr = 15$ (dash line). Here initial film profile $\delta(x) = 1$, sheet velocity $U = x$, $\varepsilon = 0.05$, $S = 2$, $Fr = 2$, $Bi = 1$, $M_w = 10$ and time $t = 1.2$.

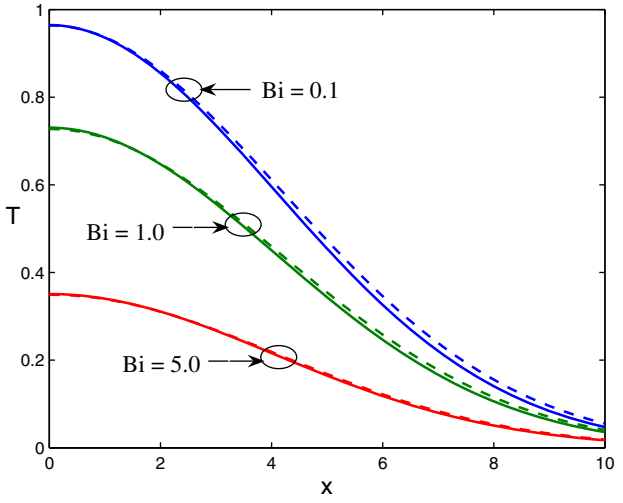

Fig. 11. Free surface temperature T versus x at $t = 1.0$ for $Pr = 1$ (solid line) and 15 (dash line), and for different Bi. Sheet temperature $\Theta = e^{-x^2/33}$, initial film profile $\delta(x) = 1$, sheet velocity $U = x$, $\varepsilon = 0.05$, $S = 2$, $Fr = 2$ and $M_w = 10$.

for stretching sheet velocity and temperature field. Further we have relaxed the planarity condition of the liquid film by allowing the variation of the film height along the stretching direction and time. The numerical solution of the evolution equation reveals that free surface is deformed owing to thermocapillarity and the deformation is advected by the flow in the direction of stretching. With the increase values of Prandtl number Pr and Biot number Bi, the temperature difference in the stretching direction decreases as a result the influence of the thermocapillarity is less pronounced at higher values of Pr and Bi.

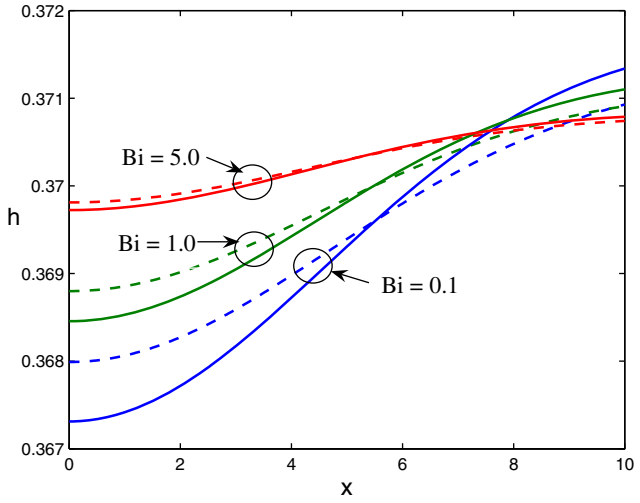

Fig. 12. Film profile h versus x at $t = 1.0$ for $Pr = 1$ (solid line) and 15 (dash line), and for different Bi. Sheet temperature $\Theta = e^{-x^2/33}$, initial film profile $\delta(x) = 1$, sheet velocity $U = x$, $\varepsilon = 0.05$, $S = 2$, $Fr = 2$ and $M_w = 10$.

Acknowledgments

The first author is grateful to The University Grants Commission, New Delhi, India for providing Teacher Fellowship (vide memo no. F.TF.W4-002-02/06-07(ERO)) and the College Authority of Jangipur College, Murshidabad, W.B., India for granting the leave during the period of work.

References

[1] L.J. Crane, Flow past a stretching plate, Z. Angew. Math. Phys. (ZAMP) 21 (1970) 645–647.
[2] H.I. Andersson, J.B. Aarseth, B.S. Dandapat, Heat transfer in a liquid film on an unsteady stretching surface, Int. J. Heat Mass Transfer 43 (2000) 69–74.
[3] C.Y. Wang, Liquid film on an unsteady stretching surface, Q. Appl. Math. 48 (1990) 601–610.
[4] B.S. Dandapat, B. Santra, H.I. Andersson, Thermocapillarity in a liquid film on an unsteady stretching surface, Int. J. Heat Mass Transfer 46 (2003) 3009–3015.
[5] C.H. Chen, Marangoni effects on forced convection of power-law liquids in a thin film over a stretching surface, Phys. Lett. A 370 (2007) 51–57.
[6] B.S. Dandapat, B. Santra, K. Vajravelu, The effects of variable fluid properties and thermocapillarity on the flow of a thin film on an unsteady stretching sheet, Int. J. Heat Mass Transfer 50 (2007) 991–996.
[7] B.S. Dandapat, A. Kitamura, B. Santra, Transient film profile of thin liquid film flow on a stretching surface, Z. Angew. Math. Phys. (ZAMP) 57 (2006) 623–635.
[8] B.S. Dandapat, S. Maity, Flow of a thin liquid film on an unsteady stretching sheet, Phys. Fluids 18 (2006) 102101.
[9] B. Santra, B.S. Dandapat, Thin film flow over a nonlinear stretching sheet, Z. Angew. Math. Phys. (ZAMP) (2008) (accepted for publication).
[10] P.M.J. Trevelyan, S. Kalliadasis, Wave dynamics on a thin-liquid film falling down a heated wall, J. Eng. Math. 50 (2004) 177–208.
[11] P.M.J. Trevelyan, B. Scheid, C. Ruyer-Quil, S. Kalliadasis, Heated falling films, J. Fluid Mech. 592 (2007) 295–334.
[12] A. Oron, S.G. Bankoff, Dynamics of a condensing liquid film under conjoining/disjoining pressures, Phys. Fluids 13 (2001) 1107–1117.